

Energetic and exergetic assessment of solar and wind potential maps in Europe

Olivier Le Corre*

Department of Energetics and Environmental Engineering,
Ecole des Mines de Nantes,
4 rue A. Kastler, BP 20722,
F-44307 Nantes cedex 3,
France

Olivier.Lecorre@mines-nantes.fr

* Corresponding author

Jean-Sébastien Broc

Department of Energetics and Environmental Engineering,
Ecole des Mines de Nantes,
4 rue A. Kastler, BP 20722,
F-44307 Nantes cedex 3,
France

Jean-sebastien.Broc@mines-nantes.fr

Ibrahim Dincer

Faculty of Engineering and Applied Science,
University of Ontario, Institute of Technology,
2000 Simcoe Street North, Oshawa, Ont., Canada L1H 7K4
Ibrahim.Dincer@uoit.ca

Biographical notes:

Olivier Le Corre is an Associate Professor of Mechanical Engineering in the Department of Energetics and Environmental Engineering at Ecole des Mines de Nantes. He has authored and co-authored refereed journal and international conferences and taken out numerous patents. He is an active reviewer for international journal.

Jean-Sébastien Broc has a PhD in energy engineering (Mines ParisTech), with a focus on evaluation of energy efficiency activities. He is a research fellow at Ecole des Mines de Nantes. His activities aim at interdisciplinary research about energy issues, crossing engineering and social sciences. He has been the expert nominated by France for the bottom-up working group of the Energy Demand Management Committee (Directive 2006/32/EC), and was also involved in CEN Task Force 190 on the standardization of energy savings calculation. He is reviewer for Energy Efficiency (Springer Ed.) and has been in the scientific committee of two international conferences.

Ibrahim Dincer is a Full Professor of Mechanical Engineering in the Faculty of Engineering and Applied Science at UOIT. Renowned for his pioneering works in the area of sustainable energy technologies, he has authored and co-authored many books and book chapters, refereed journal and conference papers, and technical reports. He has chaired many national and international conferences, symposia, workshops and technical meetings. He has delivered many keynote and invited lectures. He is a recipient of several research, teaching and service awards.

Abstract

This paper deals with a physics-based assessment of renewable energy potential in Europe, particularly solar and wind, using two literature models. A sensibility analysis with the weather data is first-done. Actual temperature, pressure, RH, global radiation and wind speed data are employed to develop energy and exergy maps for Europe, based on iso-area of land-use. These maps are compared with similar existing ones. Good agreement is obtained. A paradoxical result is obtained for wind exergy efficiency. The yearly average exergy efficiency where wind speed is less than 5 m/s is greater than the one where wind speed is greater than 7 m/s. This can be explained by the “dome” shape of wind exergy efficiency. A solar efficiency map for Europe is also developed and is a guide for choosing a renewable energy based on yearly energy production.

Keywords: Renewable Energy, Solar, Wind, Exergy, Energy, Efficiency, Map.

1 Introduction

Nowadays, European Union is considering renewable resources as major components of future energy mix and has set more and more stringent objectives (see EC2009). Renewable resources can be segmented by their converters: sun power (thermal or electric), wind power, tide power, geothermic, hydraulic and bio-fuels. Clean energy cluster must be chosen carefully and in relation with local context and constraints. Lovejoy (1996) described the necessity of solar energy as regards population, finite resources (fossil or nuclear fuels) and pollution. Use of renewable resources must challenge the intermittent production and a time gap between production and consumption, see Sovacool (2009). Hoicka and Rowlands (2011) have proposed to view solar and wind as complementary resources. Exergy analysis is a smart tool for comparison between these different applications from a thermodynamic point of view, providing a more relevant insight about the energy losses than an energy analysis (Dincer 2002). Koroneos et al. (2003) have compared numerous types and uses of energy solutions (Solar/Thermal, Wind/Electric, Geothermal, Solar/Electric and other non renewable associations) using exergy analysis. They have essentially introduced the following:

- The energy consumed in order to construct the plant, also called energy invested.

- The energy produced, also called output energy.
- The net energy produced is the difference between output energy minus energy invested.
- The input energy is the primary energy, for example the energy received by the collectors in case of solar thermal power systems, or the geothermal fluid energy in case of geothermal power plants, and so on.

They also concluded the association Solar/Thermal has the best ratios compared to other solutions: Net Energy Produced to Energy Invested and Output Energy to Input Energy.

Renewable resources (solar, wind and bio-fuels) can be seen as rival solutions requiring ground, except off-shore installation. Table 1 summarizes their respective advantages and drawbacks, see Kreith and Goswami (2007). Nevertheless, bio-fuels are still a controversial solution since there is a risk of using the food resources to produce the bio-fuels (Gasparatos et al. 2011). Consequently, we chose not to include this solution in this paper.

Renewable sources can be considered in off-grid applications, often associated with a diesel engine see Akyuz et al. (2009, 2011, 2012a), or connected to a national grid, considered as an electric “well”, as in this paper.

The main aim of this paper is to define the exergy efficiency of solar and wind converters over Europe as regards yearly production with an iso-area of land-use Based on the literature review presented in section 2, the paper proposes two converter models, one for each renewable resource (Joshi et al. 2009, and Pedersen et al. 1992). Meanwhile, a study of sensibility is performed with relevant weather inputs (temperature, pressure, RH, global radiation, wind speed). Yearly energy and exergy production maps are then established over Europe and discussed in section 4. Such maps can be a useful tool for cost analysis. Weather DOE database (Department of Energy, USA) available online is the source to build a “typical” year for 8,760 representative hours over 20 years.

Furthermore, the paper focuses on the physics (thermodynamics) underlying the energy options, in order to assess and compare their theoretical potentials according to exergy and energy indicators. The aim is to provide an objective basis upstream to the decision-making process, where the constraints specific to given projects would be taken into account additionally in further stages (e.g., land use, visual impact, noise, infrastructure requirements, etc.). Moreover, while the European Union has set targets for renewable energy production at the European level, each Member State may implement its own policies to meet its goals. Therefore, the economic and regulatory conditions (regulations, incentives, etc.) vary from one country to the other. These aspects are thus not included in our analyses either. This is indeed the topic for another field of literature (see e.g., Johansson and Turkenburg 2004, Jäger-Waldau 2007).

Nevertheless, over Europe, it can exist areas where the competition between solar and wind energy can be effective in terms of yearly electric production; next the previous considerations can take place. For example in France, the common idea is: wind turbines are always a better solution in term of electric production and when constraints appear, you can resort to PV cells.

Table 1: Advantages/Drawbacks of wind turbines and PV cells

2 METHODOLOGICAL BACKGROUND

Several authors have developed exergy model to analyse renewable energy systems. For example, Sahin et al. (2006a and 2006b) have defined an exergy model of wind turbine systems and provided a spatio-temporal wind exergy map based on a dedicated description. Pope et al. (2010) have extended this approach by taking into account the type of wind turbines (horizontal or vertical axis). In parallel, Joshi et al. (2009) have proposed a model for a photovoltaic thermal system. They have also explained their methodology in terms of exergy analysis and weather dependences. This section reviews the theoretical background of these models and perform sensitivity analyses for the weather parameters in order to classify them according to their order of influence on the exergy efficiency.

2.1 Solar energy option

The exergy of global solar radiation can be performed as Jeter (1981) proposes:

$$\dot{E}x^s = \left(1 - \frac{T_{amb}}{T_{sun}}\right) \phi_s A_{cell} \quad (1)$$

This exergy amount is spread out into an electric power and a thermal power. Electrical power is deduced as proposed by Joshi et al. (2009):

$$\dot{E}x_e^s = \eta_{cell} \dot{E}x^s \quad (2)$$

The electric efficiency η_{cell} depends on the technology (crystalline or thin film, cell or module), see web site of University of Michigan. We use 12% as a default value, and we define its theoretical limit when comparing PV cell and HAWT, see section 4.3.

There are two possibilities for the estimation of thermal power \dot{Q}_{cell} , either by considering heat transfer as a function of wind speed, see Akyuz et al. (2012b) or by enthalpy balance based on mass flow rate of the flowing air (cooling system), see Joshi et al. (2009). For ensuring the model homogeneity, the thermal power \dot{Q}_{cell} is calculated with Joshi's approach:

$$\dot{Q}_{cell} \approx \dot{m}_a C_{p_a} (T_{cell} - T_{amb})$$

where T_{cell} is estimated from Skoplaki et al. (2008) relation:

$$T_{cell} = T_{amb} + k \phi_s \quad (3)$$

Here k is the Ross coefficient and its value ranges from 0.021 (for free standing PV array mounting) to 0.054 (for opaque PV surface), see Skoplaki et al. (2008). Joshi et al. (2009) have used a k -value of 0.054 as the PV/T surface considered in their study was opaque. Since the correlation is simple and links T_{cell} with the ambient temperature and the incident solar radiation flux, it is appropriate for the prediction of the cell temperature, in a range of ambient temperature of [20-35 °C], that means a range of cell temperature of [50-80 °C]. Consequently, the thermal exergy rate of PV cell is defined as

$$\dot{Ex}_{th}^s = \left(1 - \frac{T_{amb}}{T_{cell}}\right) \dot{Q}_{cell} \quad (4)$$

The thermal exergy efficiency ψ_{th}^s is given by $\psi_{th}^e = \frac{\dot{Ex}_{th}^s}{\dot{Ex}^s}$. Then, PV cell exergy efficiency can be defined as

$$\psi^s = \frac{\dot{Ex}_e^s + \dot{Ex}_{th}^s}{\dot{Ex}^s} = \eta_{cell} + \frac{\left(1 - \frac{T_{amb}}{T_{cell}}\right) \dot{Q}_{cell}}{\left(1 - \frac{T_{amb}}{T_{sun}}\right) \phi_s A_{cell}} \quad (5)$$

Exergy efficiency of PV cell is decomposed by its electrical and thermal parts (using Joshi's model). Hence these exergies are plotted versus ambient temperature, see figure 1, and versus global solar radiation, see figure 2.

The higher the ambient temperature, the lesser the thermal exergy efficiency is, and consequently the lesser the total exergy efficiency is (by assuming that global solar radiation is constant), but this effect can be classified as a second order. For example, ambient temperature in the range of [0-30 °C] involves a variation on total exergy efficiency in the "reverse" range of [32%-30%].

The higher the global solar radiation, the higher the thermal exergy efficiency is, and consequently the higher the total exergy efficiency is (by assuming that ambient temperature is constant). This effect is classified as a first order. For example, direct radiation in the range of 50-650 Wh m⁻² involves a variation on total exergy efficiency in the range of [13%-37%].

Figure 1: Exergy efficiency for PV cell (Joshi's model): ambient temperature effect

Figure 2: Exergy efficiency for PV cell (Joshi's model): global solar radiation effect

2.2 Wind energy

Wind kinetic energy is converted to electrical power by moving a wind turbine. Consequently, the instantaneous pressure drop ΔP , between upstream and downstream of the wind

turbine, can be modelled as two thermodynamic states, denoted by the subscript 1 for upstream and 2 for downstream.

$$\Delta P(t) = P_1(t) - P_2(t) \quad (6)$$

Let's assume that firstly the linear turbine speed, noted V , is the average between up- and down-stream:

$$V = \frac{V_1 + V_2}{2} \quad (7)$$

and secondly $\frac{V_2}{V_1}$ is small.

Then, by using the Barré de St Venant equation, one can write by neglecting enthalpy variations:

$$\frac{P_1}{\rho} + \frac{V_1^2}{2} = \frac{P_2}{\rho} + \frac{V_2^2}{2} \Rightarrow V^2 = \frac{2}{\rho} \Delta P \quad (8)$$

Sahin et al. (2006a) have described a wind turbine model by adapting the wind chill temperature to this application:

$$T_{windchill,i} = 35.74 + 0.6215 T_a - 35.75 V_i^{0.16} + 0.4274 T_a V_i^{0.16} \quad (9)$$

where $i \in \{1, 2\}$.

Thermodynamic states and specific "thermodynamic" exergy function of wet air are detailed by Dincer and Rosen (2007):

$$ex^{th} = (Cp_a + \omega Cp_v) T_0 \left[\left(\frac{T}{T_0} \right) - 1 - \ln \left(\frac{T}{T_0} \right) \right] + (R_a + R_v \omega) T_0 \ln(P / P_0) + T_0 \left[(R_a + R_v \omega) \ln \left(\frac{R_a + R_v \omega_0}{R_a + R_v \omega} \right) + R_v \ln \left(\frac{\omega}{\omega_0} \right) \right] \quad (10)$$

with R_a the air gas constant ($R_a = 287 \text{ J / kg K}$), R_v the water gas constant ($R_v = 461.5 \text{ J / kg K}$), Cp_a the specific heat of air (1002 J/kg K) and Cp_v the specific heat of vapour at reference temperature (1869 J.kg/K at 25°C). Subscript 0 refers to dead state corresponding to ambient conditions; see Gaggioli (2012) or Sogut et al. (2009).

Then, exergy function is

$$Ex^{th} = \dot{m} ex^{th} \quad (11)$$

where the specific humidity ratio:

$$\omega = \frac{\dot{m}_w}{\dot{m}} \quad (12)$$

where \dot{m} is obtained with the continuity equation:

$$\dot{m} = \rho A_W V \quad (13)$$

Golding (1955) has established the maximum power \hat{W} that can be extracted for given weather conditions:

$$\hat{W} = \frac{8}{27} \rho A V_1^3 \quad (14)$$

Horizontal-axis wind turbines (HAWT), a more realistic model for power \dot{W} , is provided by Pedersen et al. (1992), see figure 3. This model of electric power versus wind speed is proposed for an optimal pitch angle and angle of attacks, see Thumthae and Chitsomboon (2009) for their definitions. To omit the wind direction, the authors assume that HAWT is equipped with yaw bearing system and untwisted blade. HAWT features are: rotor diameter 18m, hub length 30m, nominal power 100 kW.

Figure 3: Electric power versus wind speed for HATW (Pedersen's model)

The electric efficiency of wind turbine is defined by the ratio between its power and its maximum power and is plotted in figure 4:

$$\eta = \frac{\dot{W}}{\hat{W}} \quad (15)$$

It is very important to highlight that such a wind turbine has its maximum electric efficiency for a wind speed of around 8 m/s. Beyond this limit the power increases with wind speed but the efficiency decreases.

Then, wind exergy efficiency can be defined as:

$$\psi^w = \frac{\dot{W}}{\Delta \left(\frac{1}{2} \dot{m} V^2 + Ex^w \right)} = \frac{\dot{W}}{\frac{1}{2} \dot{m} (V_1^2 - V_2^2) + Ex_1^w - Ex_2^w} \quad (16)$$

Note that Hellmann equation gives the wind speed correction taking into account wind turbine hub:

$$V_{corr} = V_{meas} \left(\frac{H}{H_{meas}} \right)^\alpha \text{ with } \alpha = 0.28 \quad (17)$$

For this model, instantaneous ambient conditions are defined by: temperature, wind speed, pressure and relative humidity. Then, the weather database of DOE is required to perform the sensitivity analyses.

Energy efficiency of HATW (using Pedersen's model), see Eq (15), is plotted in Figure 4. Maximum energy efficiency, 50%, corresponds with 8 m/s. The transfer function between wind speed and electric efficiency is non linear and its shape is like a "dome": a same value of energy efficiency can correspond with a low or a high wind speed, and thus a low or high electrical power. Therefore, an analysis of HATW energy efficiency cannot be done in a straightforward manner. It requires to set first either the wind speed or the electric power.

Figure 4: Electric efficiency for HATW (Pedersen's model)

Typical values of pressure variations between upstream and downstream (ΔP as defined by eq(1)) and temperature variations are given in Table 2.

Table 2 : Pressure and temperature variations

Exergy efficiency of HATW (using Pedersen's model), see Eq (16), is plotted in Figure 5-a). The shape between exergy efficiency of HATW (Pedersen's model) and wind speed is approximately the same as previously, with its maximum exergy efficiency, around 35%, for a wind speed of 7m/s, in the specified conditions. It is worth to propose a parametric study of exergy efficiency as regards these conditions:

- Ambient temperature effect on exergy efficiency is plotted in Figure 5-b). This effect is very significant and must be associated to the wind chill temperature. This effect can be classified as a first order.
- Ambient pressure and relative humidity effects on exergy efficiency are plotted in Figure 5-c) and Figure 5-d) respectively. These effects are not significant and are classified as a second order. The slopes are $20 \cdot 10^{-6}$ for ambient pressure and $-4.6 \cdot 10^{-8}$ for relative humidity.

Figure 5: Exergy efficiency for HATW (Pedersen's model): a) wind speed effect, b) ambient temperature effect, c) ambient pressure effect, and d) relative humidity effect.

3 CASE STUDY FOR EUROPEAN UNION

Using Joshi's model for PV cells and Pedersen's model for HATW, we computed the exergy efficiency for average weather conditions of a set of locations across Europe. As an example, data and results (exergy efficiencies for PV cells and wind power) for Paris (France) are detailed in this section.

The models require weather data:

- wind speed
- ambient temperature
- ambient pressure
- global radiation
- relative humidity

These data are available on DOE website for various meteorological stations and for a "representative" year with its 8760 hours. This choice requires more CPU-time than monthly

data, but it avoids introducing additional uncertainties due to the estimation of data distribution, see Coskun et al. (2011).

An assumption was also needed to take into account the difference in the land use for both systems (solar PV and wind power). A usual building layout of wind turbines is a separation of at least around 5 times the rotor length to avoid fluid mechanic interactions. Then, in this study, the authors have considered that the PV cell area is 5 times the cross area of the wind turbines, that is to say 1,200m². Cumulative energy or exergy have been calculated for this surface.

The exergy efficiency defined from Joshi's model for PV cells is a function of ambient temperature and direct radiation, see figure 6. As explained before, ambient temperature has a second order effect, then the main relation between this exergy efficiency and global radiation is mostly independent of ambient temperature.

Figure 6: Total exergy efficiency of PV cell versus direct radiation for Paris

The wind speed over 8760 hours is plotted in Figure 7-a): the wind speed range is [0-20] m/s. Statistical tools are commonly used to analyse such data: the cumulative normal distribution of hourly wind speed in interval $[v_j; v_{j+1}]$ is the number of times that the hourly wind speed (based on DOE database) occurs in this interval over the year. Same procedure is applied to wind power. Figure 7-b) gives information about cumulative normal distributions of hourly wind speed (see Kantar and Usta (2008), Ulgen and Hepbasli (2002)) and its associated wind power. These distributions show clearly the gap between hourly distribution and power distribution, hence 25% of the energy is produced only during 3% of the year where the wind speed is 11 m/s. Such a gap was well expected, see Chang (2010). Monthly wind direction is showed for three months (January, May and June) and reveals very large orientation discrepancies, see Figure 7-c).

Figure 7: a) Representative year of wind speed for Paris
b) Cumulative normal distribution of wind speed and its associated wind power for Paris
c) Monthly wind direction for three months (January, May and June) for Paris

In this study, authors assume that HAWT are well oriented as regards wind distribution. The monthly average temperatures are plotted in figure 8-a), and its range is [3-25]°C. The monthly direct radiation is plotted in figure 8-b).

Figure 8: a) Monthly ambient temperature at Paris
b) Monthly direct radiation at Paris

The exergy efficiency for HAWT (using Pedersen's model) is a function of ambient conditions as well. But there are crossed effects not so obvious. In Figure 9, the wind exergy efficiency is plotted (for Paris):

- versus wind speed: as expected, the faster the wind speed, the greater the wind exergy, but this observation is within an envelope: this shape shows a first order effect, see Figure 9-a).
- versus ambient temperature: an upper linear limit seems to exist. There is a significant scattering then these coupled effects are important, see Figure 9-b).
- versus ambient pressure: this parameter has a second order effect, then no tendency can be proposed, see Figure 9-c).
- versus relative humidity: same comment as for ambient pressure, see Figure 9-d).

Figure 9: Hourly exergy efficiency of HAWT

- a) versus wind speed
- b) versus ambient temperature
- c) versus ambient pressure
- d) versus relative humidity

More than 100 meteorological stations have been considered, see figure 10, to represent Europe. Spline interpolation is performed with common Sandwell algorithm (1987).

Figure 10: Location of meteorological stations over Europe

4 RESULTS AND DISCUSSION

4.1 Primary exergy

By "primary exergy", authors mean the exergy amount: this amount is calculated by eq (4) for solar resources, and by eq (11) for wind resources. A cumulative amount is then computed over the year, see Figures 11.

- The European Commission's Joint Research Centre in Ispra published an interactive map of Europe (and Africa) showing the photovoltaic solar electricity potential, see EC website. Figure 11-a) shows the latitude 45° as a good limit. Two singular locations must be underlined: one near London (UK) and a second one near Göteborg (Sweden).
- An European Wind Atlas has been published for the European Commission by the Risø National Laboratory, see EWA website. Wind "primary exergy" is very significant on the west coast and especially in Ireland, see figure 11-b). On Mediterranean coast, an important wind, called "mistral", blows near Marseille (France). EWA wind zones have been plotted in dotted lines in Fig 11-b). These zones have a good concordance with these obtained by our computations.

Figure 11: Primary exergy from a) sun and b) wind resources

4.2 Real conversion

Cumulative electric power is performed from eq (2) for sun resource and by using eq (15) for wind resource (with weather inputs from DOE database).

- For sun resource, real cumulative electric power is plotted in Figure 12-a). With an electric efficiency of 12%, the maximum cumulative electric power is only 240 MWh/y, under the latitude 45°.
- For wind resource, real cumulative electric power is plotted in Figure 12-b). In this configuration, the maximum cumulative electric power is around 600 MWh/y. Its electric conversion benefits from the number of hours of availability for the considered resource.

Figure 12: Yearly electric production a) solar resource b) wind resource

Electric energy predicted from wind resource versus sun resource for each meteorological station is plotted in Figure 13. On this plot, the first bisectrix line has been added and y-axis has been reshaped. Below this bisectrix line, one can determine few stations (in Austria: Innsbruck and Linz, in Italia: Messina, Valence and Venice, in Slovakia: Brastilava, in Spain: Valencia, and in Roumania: Cluj and Constanta) where sun resource could be interesting in term of electric energy.

Figure 13: Wind energy potential versus sun energy potential for the 100 meteorological stations tested

Exergy efficiencies are then detailed as follows:

- Solar exergy efficiency, averaged over the year, is calculated from eq (5) and plotted in figure 14-a). Since electrical efficiency is taken as 12%, this plot shows that “thermal exergy efficiency” is in the range [5-15]%. A point worth mentioning here is that the combined heat and power production from a PV/T system would increase the usability of the system. Also a good electrical efficiency can be maintained throughout the day as the thermal exergy from the system would have affected the latter adversely otherwise removed from the PV panels.
- Wind exergy efficiency, averaged over the year, is calculated from eq (16) and plotted in Figure 14-b). This plot must be very carefully read because HAWT exergy efficiency against wind speed is roughly a parabolic shape (see figure 5-a)). Indeed, the maximum exergy efficiency is obtained for a wind speed around 7m/s. while the maximum electric production is achieved for 13.5m/s. In other words, West Ireland coast can produce the

greater amount of electricity but its exergy efficiency is lower than other places (where the wind speed is closer to 7 m/s). This point underlines that wind turbines must be designed for the place where they are located. Since no heat is recoverable by this converter, wind exergy efficiency is lower than the sun one. But in practice, most of the PV systems do not recover the “waste” heat either.

Figure 14: Yearly exergy efficiency a) solar resource b) wind resource

4.3 Solar/Wind electric production challenge

As shown in the previous results, solar resource is more penalized by its intermittent feature than wind resource. It is then interesting to ask: What would be the required solar electric efficiency to exceed HAWT electric production? Knowing HATW electric production and available direct radiation both cumulated over year, the ratio of both would give this solar electric efficiency theoretical threshold. Solar efficiency theoretical thresholds are plotted in figure 15 for the locations tested.

- Near North Sea coasts (France, Belgium, Germany, The Netherlands), Baltic sea coasts and UK, the solar efficiency theoretical threshold would be over 40%. 40% is beyond the current technological limits for solar efficiency, which is about 30% see MU web site. Consequently, solar production can not challenge wind production in these regions.
- Near Mediterranean Sea coast in France, wind resource called “mistral” is in competition with solar resource since real electric efficiency is nowadays technologically feasible since the solar electric efficiency theoretical threshold can be met with current technology.
- Above the latitude 45°, solar resource can already produce more electricity than wind resource.

This paper just provides a tendency, not an exact result: an assessment for a specific application is still required to go further in the decision process.

Figure 15: Solar electric efficiency theoretical threshold

5 CONCLUSIONS

Solar and wind resources have extensively been studied over Europe in terms of: available resources, real conversion, and exergy efficiency. To achieve these maps, a complete study of influencing parameters is firstly performed using two classical models (Joshi’s model for PV cells and Pedersen’s model for HATW). Global radiation is the main parameter for PV cells’ model and wind speed for HATW model. Ambient temperature is a major parameter for exergy calculations for both. Hourly weather DOE database are used for Europe and compared qualitatively to the literature data and maps. Then, we obtain with the DOE

database the maps of renewable resources over Europe. For solar resource, the latitude 45° is clearly a limit to produce a significant amount of electricity. For wind resource, 4 regions (North sea coasts, Baltic sea coasts, a specific coast of Mediterranean sea and UK) are very effective for electrical production.

To challenge wind resource by solar resource, authors have evaluated a theoretical PV electrical efficiency threshold. If one accepts a maximum value of electric conversion efficiency around 40%, the previous four regions are not effective for solar energy (whatever the technological progress). This result, more or less intuitive, is consequently established on a thermodynamic point of view with the DOE weather database without any cost consideration. Renewable energy is sometimes more ideological than scientific. Then this kind of study could be complete by economic and regulatory conditions (regulations, incentives, etc.) to be useful for decision makers.

References

- Akyuz, E., Oktay, Z. and Dincer, I. (2009) The technico-economic and environmental aspects of a hybrid PV-Diesel-battery power system for remote farm houses, *Int. J. Global Warning*, Vol. 1, pp392-404.
- Akyuz, E., Oktay, Z. and Dincer, I. (2011) Energetic, environmental and economic aspects of a hybrid renewable energy system: a case study, *Int. J. of Low-Carbon Technology*, Vol. 6, pp 44-54.
- Akyuz, E., Oktay, Z. and Dincer, I. (2012a) A case study of hybrid wind-solar power system for reduction of CO₂ emissions, *Int. J. Global Warning*, Vol. 4, pp52-67.
- Akyuz, E., Coskun, C., Oktay, Z. and Dincer, I. (2012b) A novel approach for estimation of photovoltaic exergy efficiency, *Energy*, Vol. 44, pp 1059-1066.
- Chang, T.P. (2010) Wind speed and power density analyses based on mixture Weibull and maximum entropy distribution, *Int. J. Applied Science and engineering*, Vol. 8, pp. 39-46.
- Coskun, C., Oktay, Z. and Dincer, I. (2011) Estimation of monthly solar radiation distribution for solar energy system analysis, *Energy*, Vol. 36, pp1319-1323.
- Dincer I. (2002) The role of exergy in energy policy making, *Energy Policy*, Vol. 30, pp. 137–149.
- Dincer, I. and Rosen, M.A. (2007) *Exergy: energy, environment and sustainable development*, Ed. Elsevier, ISBN: 978-0-08-044529-8.
- EC2009, Directive 2009/28/EC of 23 April 2009 on the promotion of the use of energy from renewable sources
- Gaggioli, R. A. (2012) The dead state, *Proceedings of ECOS 2012, Perugia, Italy*, pp1-13.
- Gasparatos, A., Stromberg, P, Takeuchi, K. (2011) Biofuels, ecosystem services and human wellbeing: Putting biofuels in the ecosystem services narrative, *Agriculture, Ecosystems & Environment*, Vol. 142(3–4), pp. 111–128
- Golding, E.W. (1955) *The generation of Electricity by Wind Power*, E&F N. Spon Limited: London.
- Hoicka, C.E. and Rowlands, I. H. (2011) 'Solar and wind resource complementarity: Advancing options for renewable electricity integration in Ontario, Canada', *Renewable Energy*, Vol. 36, pp. 97-107.

494 Jäger-Waldau, A. (2007) Photovoltaics and renewable energies in Europe, *Renewable and*
495 *Sustainable Energy Reviews*, Vol.11(7), pp. 1414–1437

496 Jeter, S.J. (1981) 'Maximum conversion efficiency for the utilization of direct solar radiation',
497 *Solar Energy*, Vol.26, pp. 231-236.

498 Johansson T.B, Turkenburg, W. (2004) Policies for renewable energy in the European Union
499 and its member states: an overview, *Energy for Sustainable Development*, Vol.8(1), pp.
500 5-24

501 Joshi, A. S., Dincer, I. and Reddy, B. V. (2009) 'Development of solar exergy maps', *Int. J.*
502 *Energy Res.*, Vol. 33 pp. 709-718.

503 Koroneos, C., Spachos, T. and Moussiopoulos, N. (2003) 'Exergy analysis of renewable
504 energy sources', *Renewable Energy*, Vol. 28, pp. 295-310.

505 Kreith, F. and Yogi Goswami, D. (2007) *Handbook of energy efficiency and renewable*
506 *energy*, CRC Press, ISBN 0-8493-1730-4.

507 Lovejoy, D. (1996) 'The necessity of solar energy', *Renewable energy*, Vol. 9, pp. 1138-
508 1143.

509 Pedersen, T.F., Petersen, S.M., Paulsen, U.S., Fabian, O., Pedersen, B.M., Velk, P., Brink,
510 M., Gjerding, J., Frandsen, S., Olesen, J., Budtz, L., Nielsen, M.A., Stiesdal, H.,
511 Petersen, K.Ø., Danwin, P.L., Danwin, L.J. and Friis, P. (1992). Recommendation for
512 wind turbine power curve measurements to be used for type approval of wind turbines in
513 relation to technical requirements for type approval and certification of wind turbines, in
514 *Denmark. Danish Energy Agency*, September.

515 Pope, K., Dincer, I. and Naterer G.F. (2010), 'Energy and exergy efficiency comparison of
516 horizontal and vertical axis wind turbines', *Renewable energy*, Vol. 35, pp. 2102-2113.

517 Sahin, A. D., Dincer, I. and Rosen, M. A. (2006a) *Development of new spatio-temporal wind*
518 *exergy maps*, Proceedings of ASME 2006, Mechanical Engineering Congress and
519 Exposition, Nov. 5-10, Chicago, Illinois, USA.

520 Sahin, A. D., Dincer, I. and Rosen, M. A. (2006b) 'Thermodynamic analysis of wind energy',
521 *Int. J. Energy Res.*, Vol. 30 pp. 553-566.

522 Sandwell, D. T., (1987) 'Biharmonic Spline Interpolation of GEOS-3 and SEASAT Altimeter
523 Data', *Geophysical Research Letters*, Vol. 2, pp. 139-142.

524 Skoplaki, E., Boudouvis, A.G. and Palyvos, J.A. (2008) 'A simple correlation for the operating
525 temperature of photovoltaic modules of arbitrary mounting,' *Solar Energy Materials and*
526 *Solar Cells*, Vol. 92, pp. 1393-1402.

527 Sogut, Z., Oktay, Z. and Hepbasli, A. (2009) Investigation of effect of varying dead-state
528 temperatures on energy and exergy efficiencies of a Raw Mill process in a cement plant,
529 *Int. J. Exergy*, Vol. 6, pp. 655-670

530 Sovacool, B.K. (2009) 'The intermittency of wind, solar, and renewable electricity generators:
531 Technical barrier or rhetorical excuse?', *Utilities Policy*, Vol. 17, pp. 288-296.

532 Thumthae, C. and Chitsomboon, T. (2009) 'Optimal angle of attack for untwisted blade wind
533 turbine', *Renewable Energy*, Vol. 34, pp. 1279–1284.

534 Ulgen, K. and Hepbasli, A. (2002) Determination of Weibull parameters for wind energy
535 analysis of Izmir, Turkey, *Int. J. Energy Research*, Vol. 26, pp. 495-506.

536 Website

537 DOE, <http://apps1.eere.energy.gov/buildings/energyplus/>, last access 08/09/2012

538 EC, <http://re.jrc.ec.europa.eu/pvgis/apps/radmonth.php?lang=en&map=europe>, last
539 access 08/09/2012

540 EWA, <http://www.windatlas.dk/europe/About.html> last access 08/09/2012

541 UM, http://css.snre.umich.edu/css_doc/CSS07-08.pdf, last access 08/29/2012

542

543 **Nomenclature**

544 Symbols

545	A	rotor swept area	$[m^2]$
546	A_{cell}	cell area	$[m^2]$
547	C_p	heat capacity at constant pressure	$[J\ kg^{-1}\ K^{-1}]$
548	\dot{E}_x	exergy rate	$[W]$
549	P	pressure	$[Pa]$
550	\dot{Q}	thermal power	$[W]$
551	R	specific gas constant	$[J\ kg^{-1}\ K^{-1}]$
552	T	temperature	$[K]$
553	V	speed	$[m\ s^{-1}]$
554	\dot{W}	wind turbine power	$[W]$
555	ex	specific exergy	$[J\ kg^{-1}]$
556	\dot{m}	mass flow rate	$[kg\ s^{-1}]$
557	t	time	$[s]$

558

559 Greek letters

560	Δ	difference	
561	Ψ	exergy efficiency	
562	η	energy efficiency	
563	ϕ	direct solar radiation	$[W\ m^{-2}]$
564	ρ	density	$[kg\ m^{-3}]$
565	ω	specific humidity ratio	

566

567 Subscripts

568	0	means reference conditions, i.e. ambient conditions
569	1	upstream
570	2	downstream
571	V	referred to water vapor
572	a	referred to air
573	e	electric
574	i	index
575	amb	ambient conditions
576	$cell$	solar PV cell
577	$corr$	Hellmann's correction
578	$meas$	mean measurement conditions
579	sun	sun
580	$windchill$	wind chill

581

582 Exponents

583	th	thermodynamic
584	W	wind
585	S	solar

586

587 Notation

588	\wedge	maximum
-----	----------	---------

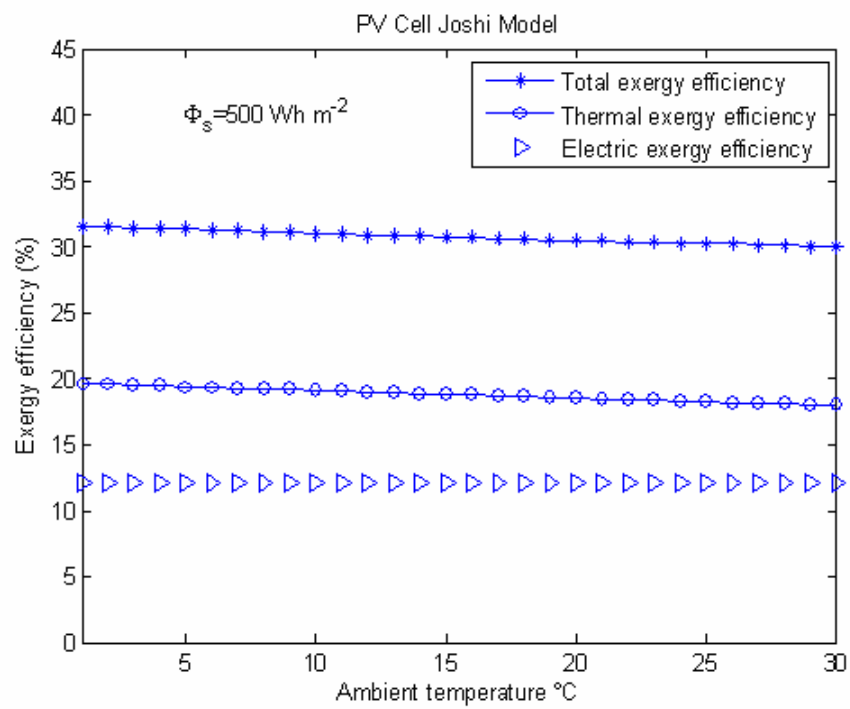


Figure 1: Exergy efficiency for PV cell (Joshi’s model): ambient temperature effect

593

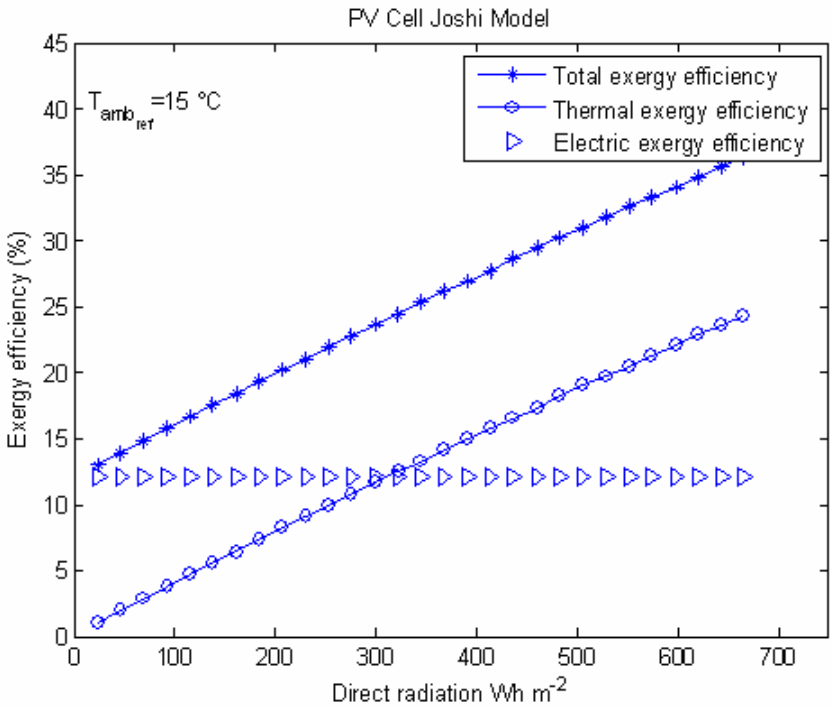


Figure 2: Exergy efficiency for PV cell (Joshi’s model): global solar radiation effect

594
595
596

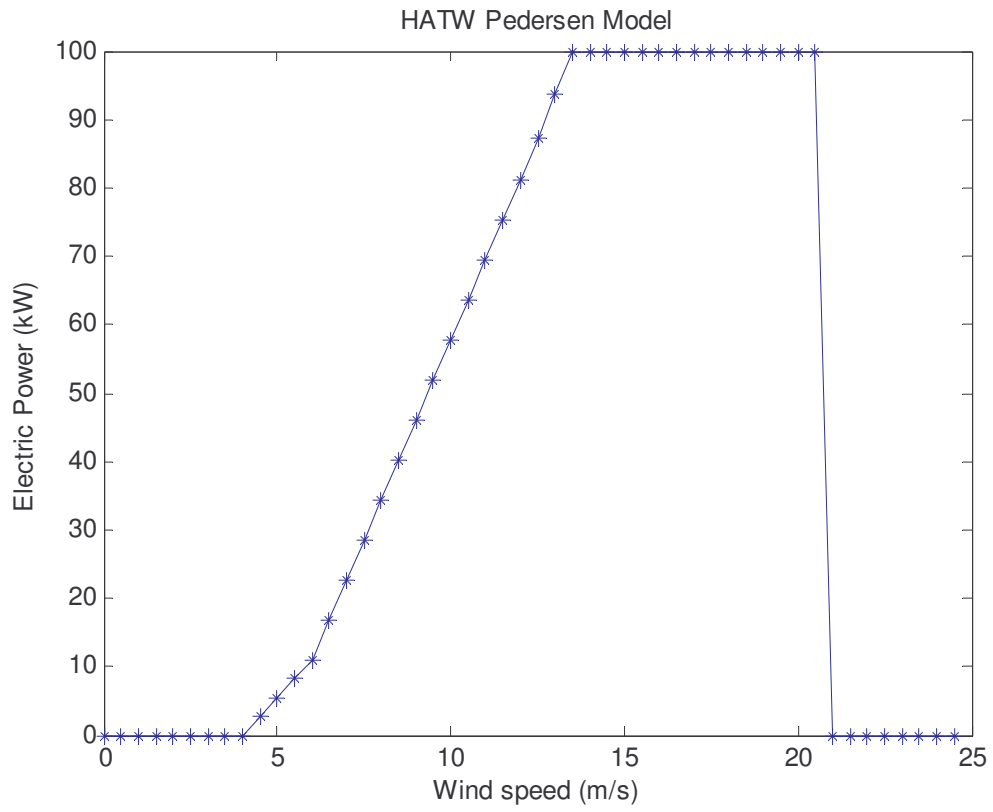


Figure 3: Electric power versus wind speed for HATW (Pedersen's model)

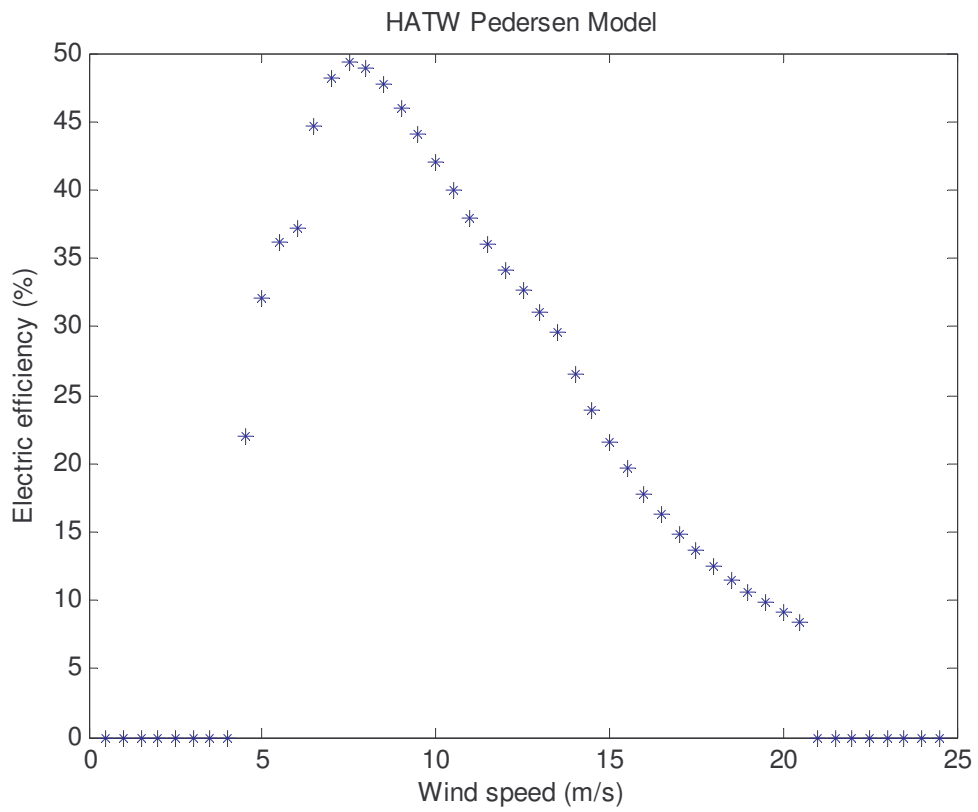
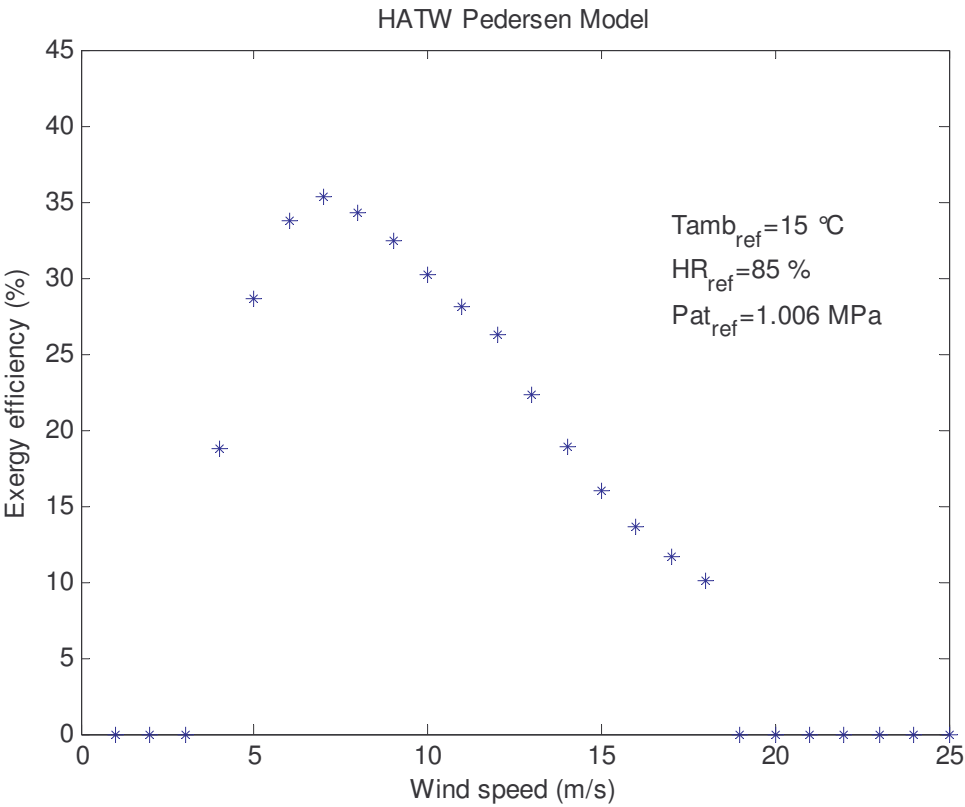
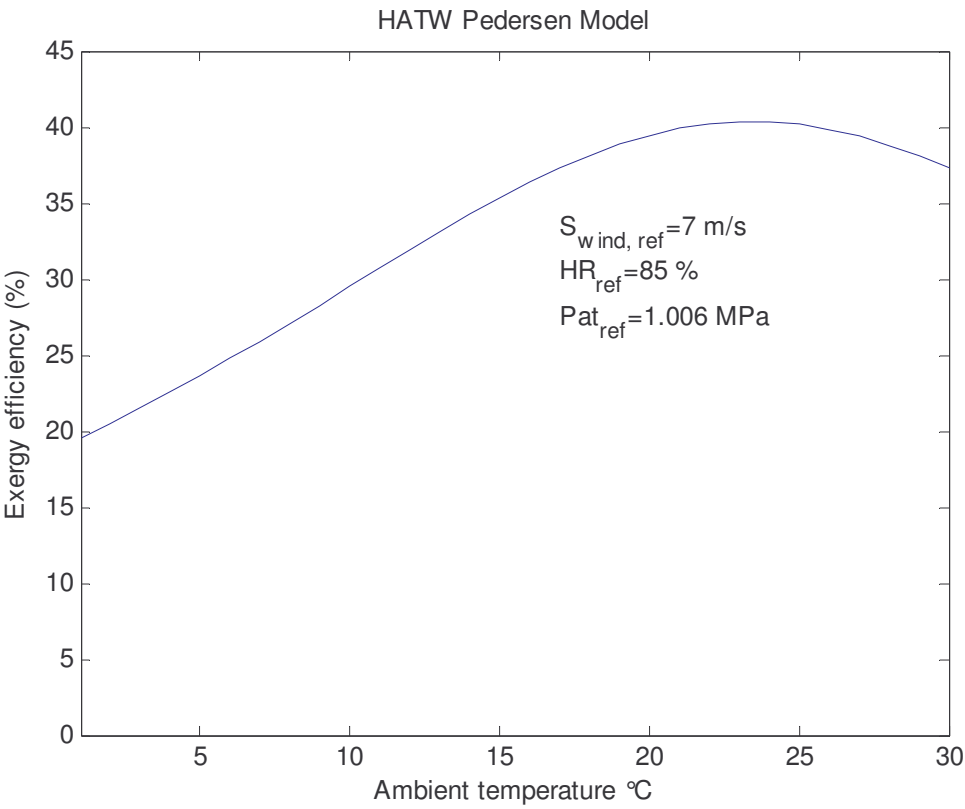


Figure 4: Electric efficiency for HATW (Pedersen's model)

601



602



603

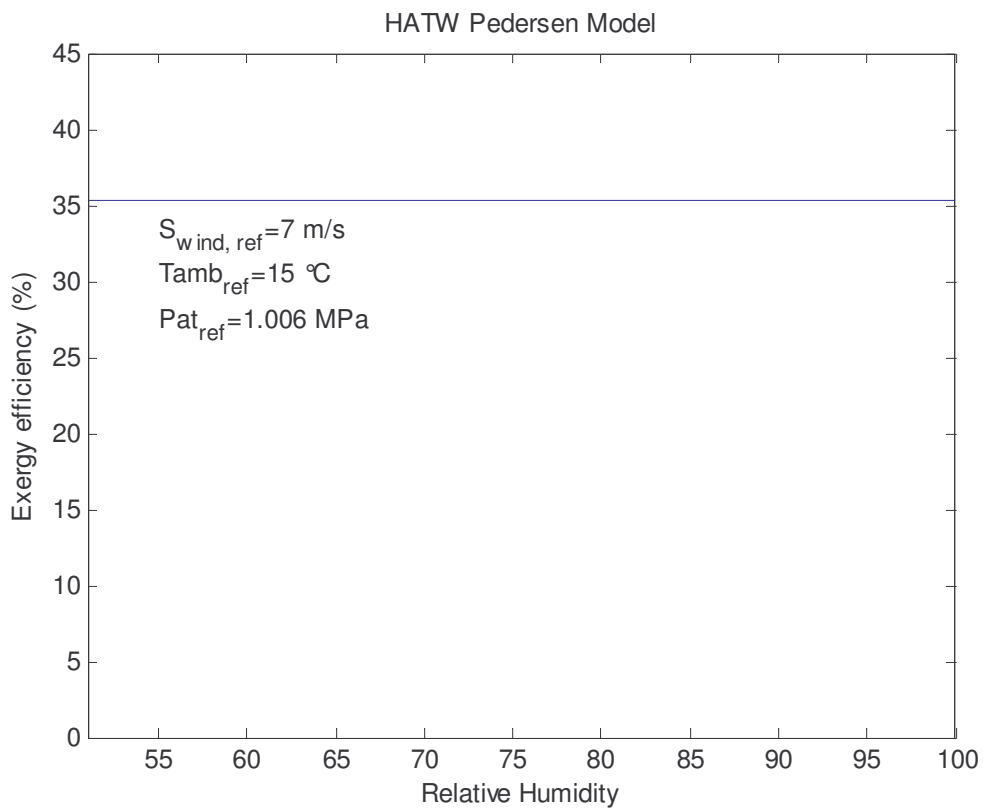
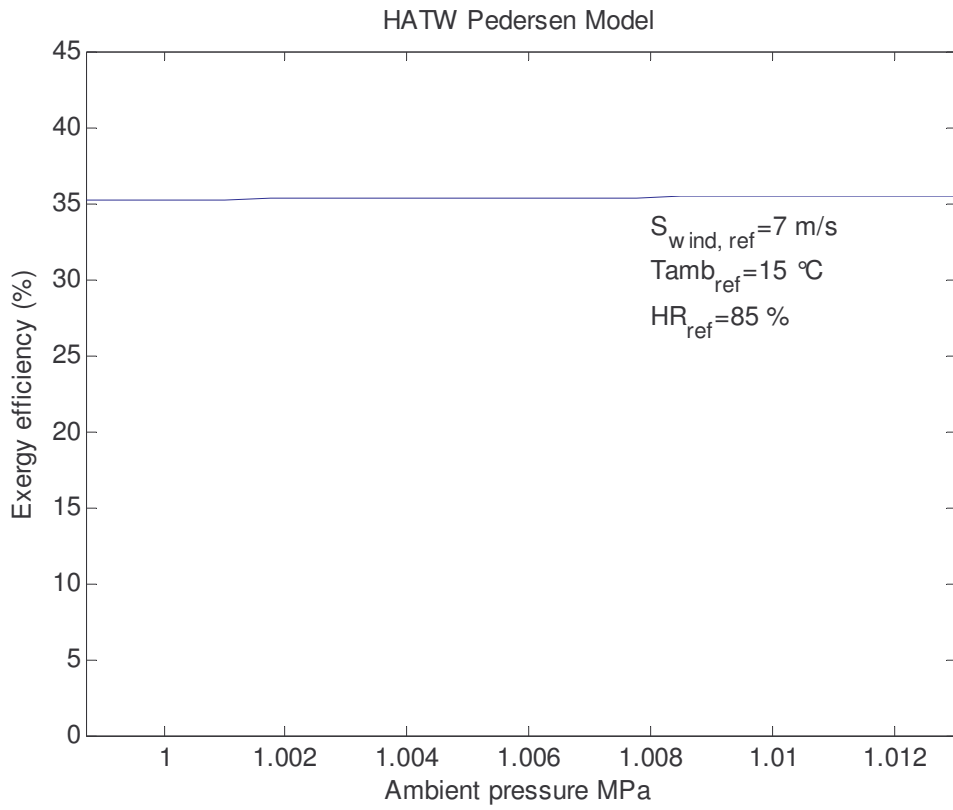
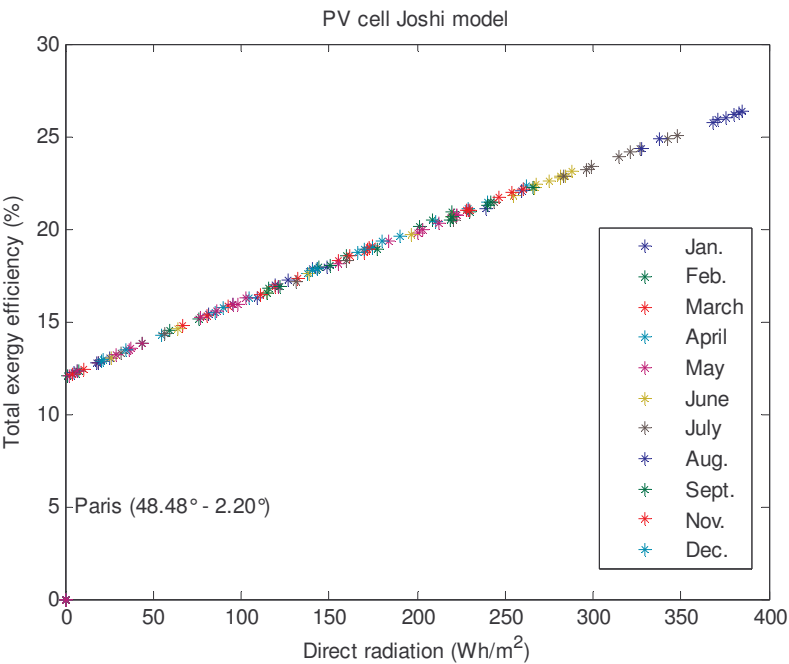


Figure 5 : Exergy efficiency for HATW (Pedersen's model): a) wind speed effect, b) ambient temperature effect, c) ambient pressure effect, and d) relative humidity effect.

610



611
612

Figure 6 : Total exergy efficiency of PV cell versus direct radiation for Paris

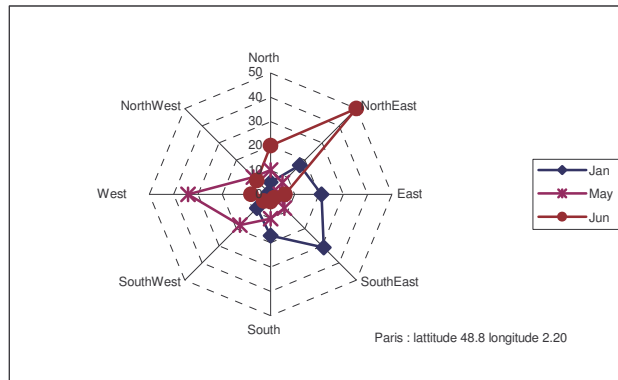
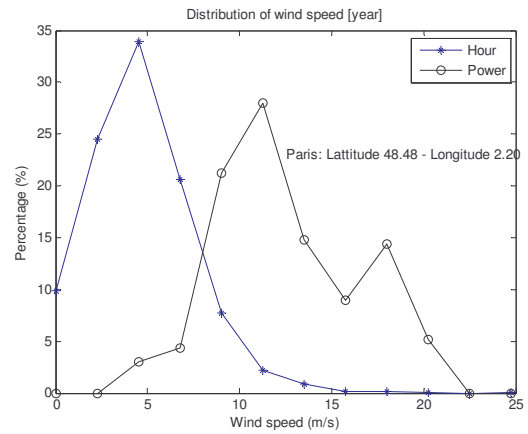
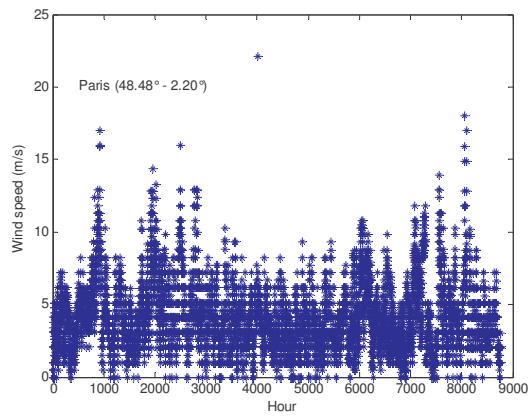


Figure 7 : a) Representative year of wind speed for Paris
b) Cumulative normal distribution of wind speed and its associated wind power for Paris
c) Monthly wind direction for three months (January, May and June) for Paris

618

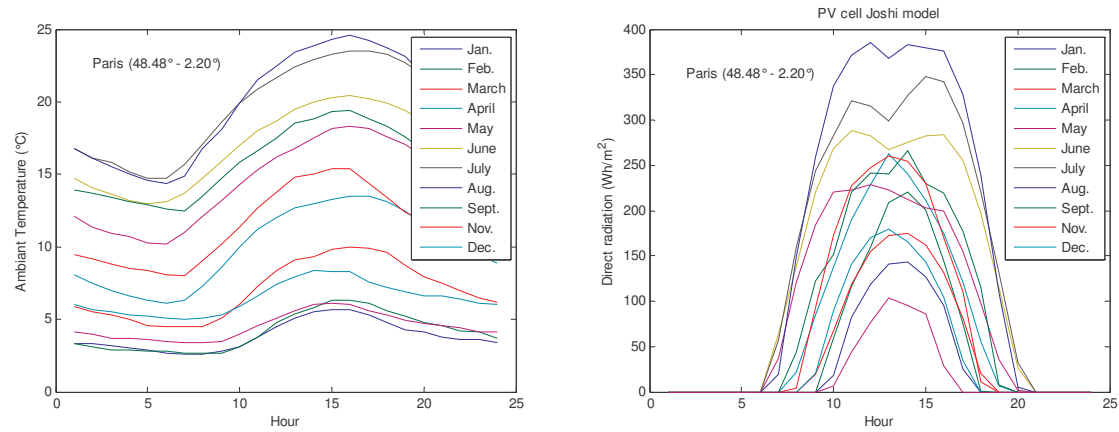
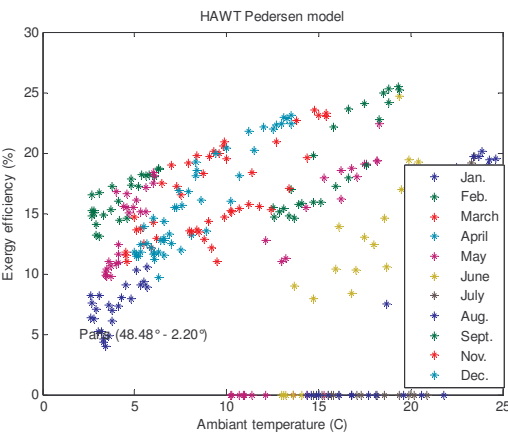
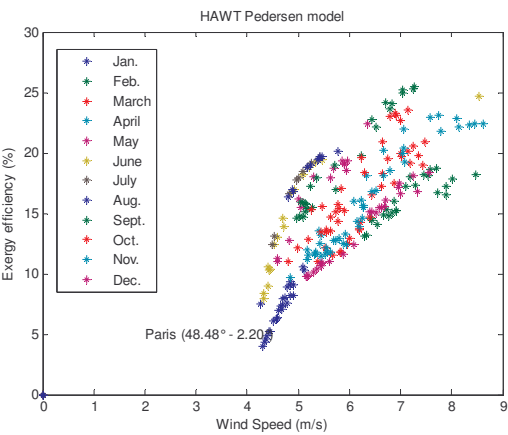


Figure 8 : a) Monthly ambient temperature at Paris
b) Monthly direct radiation at Paris

619
620
621

622



623

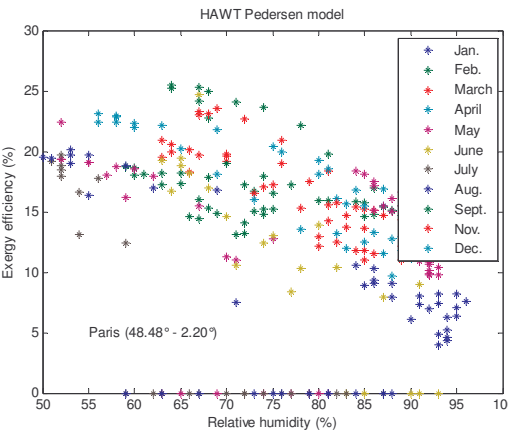
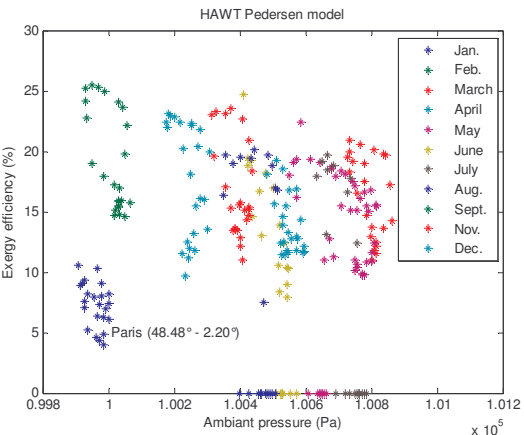


Figure 9: Hourly exergy efficiency of HAWT
a) versus wind speed
b) versus ambient temperature
c) versus ambient pressure
d) versus relative humidity

624

625

626

627

628

629

630

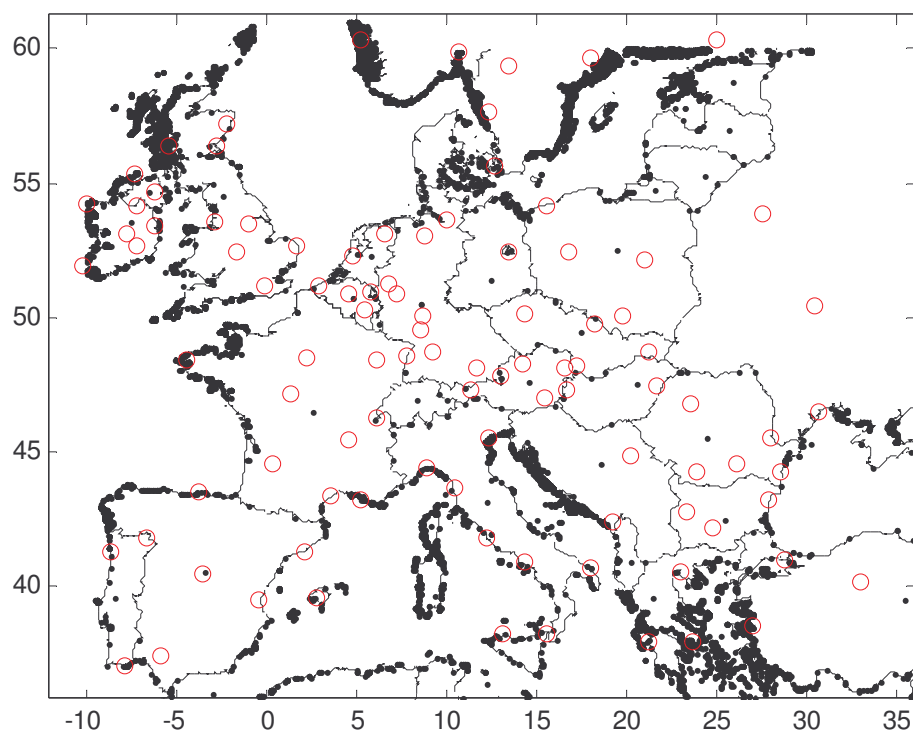


Figure 10: Location of meteorological stations over Europe

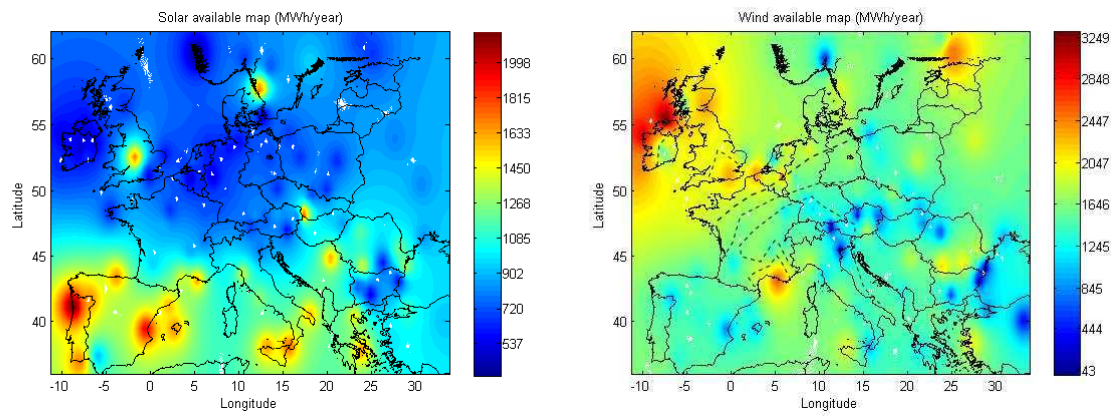


Figure 11: Primary exergy from a) sun and b) wind resources

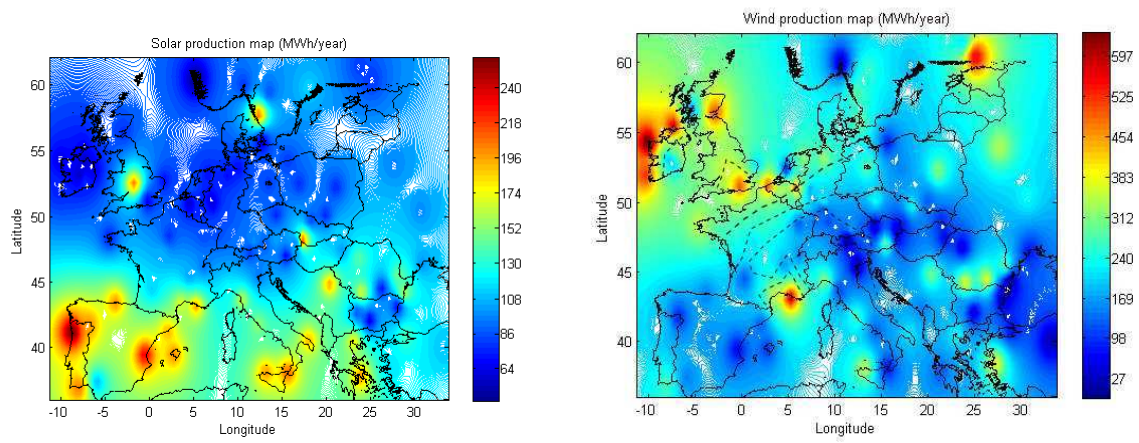


Figure 12: Yearly electric production a) solar resource b) wind resource

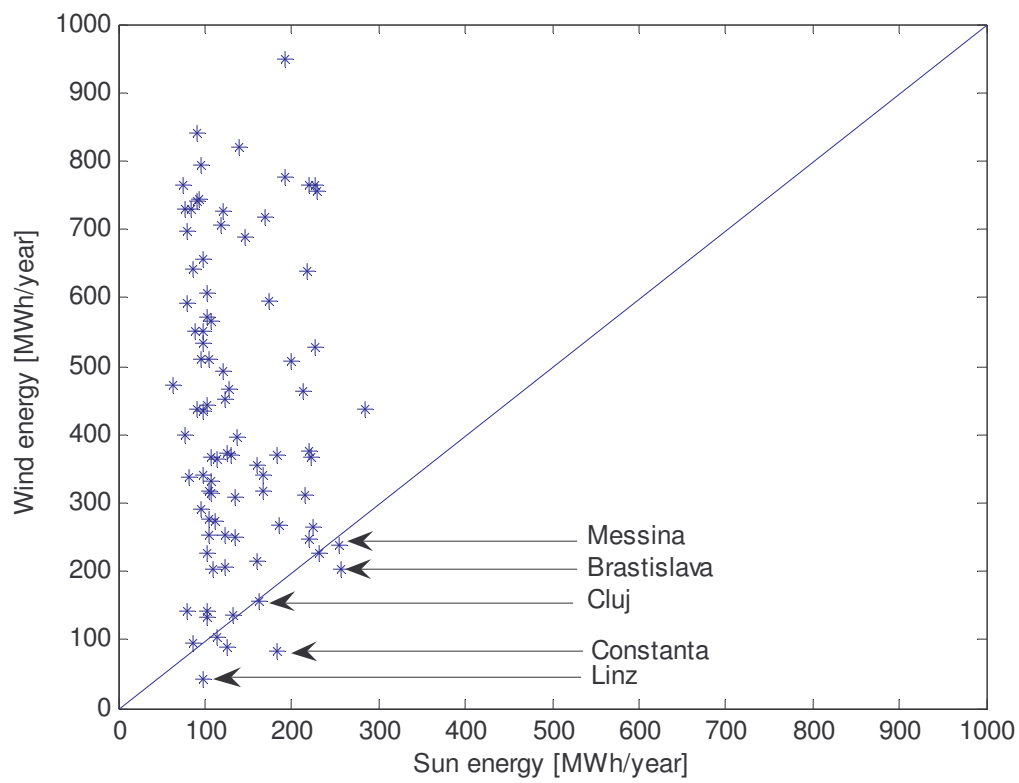


Figure 13: Wind energy potential versus sun energy potential for the 100 meteorological stations tested

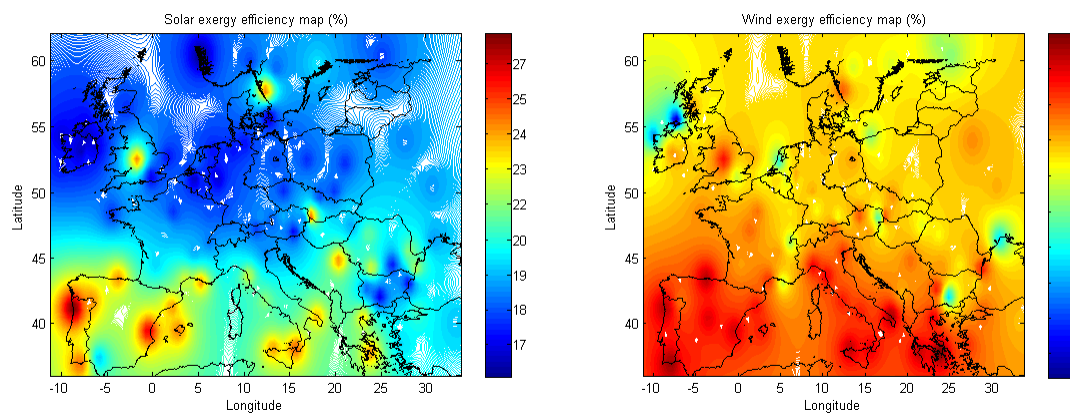


Figure 14: Yearly exergy efficiency a) solar resource b) wind resource

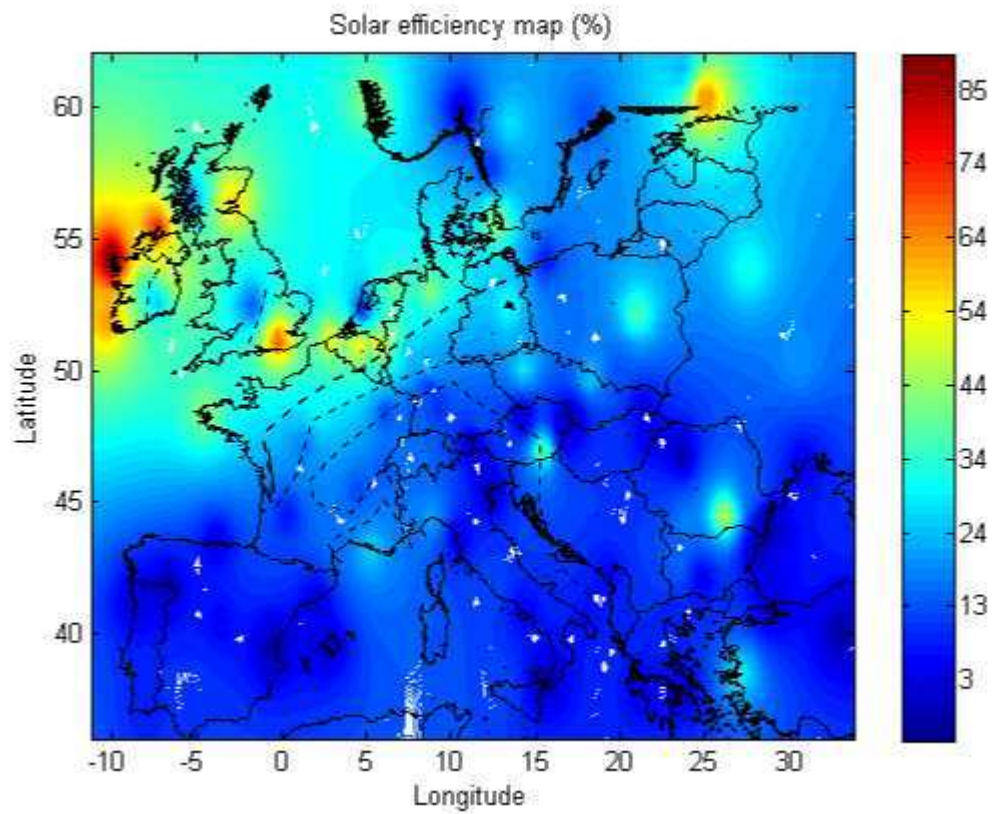


Figure 15 : Theoretical solar electric efficiency

644
645

Table 1: Advantages/Drawbacks of wind turbines and PV cells

	Advantages	Drawbacks
Renewable Resources	Freely available do not generate direct pollution	Intermittent resources: highly climate dependent
Wind Turbines	generation and maintenance are cost effective Performances are still improving	need 3 times the amount of installed capacity to meet demand noisy construction can be very expensive may affect endangered species of birds
Photo-Voltaic cells	costs are dropping performances are improving extremely durable cheap maintenance	current technologies require large amounts of land production levels can be affected by weather conditions (for example cloudy and stormy days)

646

647
648

Table 2 : Pressure and temperature variations

Wind Speed V1 [m/s]	$\Delta V=V1-V2$ [m/s]	$\Delta P=P1-P2$ [Pa]	$\Delta T=T2-T1$ wind chill [K]	HATW power [kW]
4	0.4	11.4	1.4	2.40
5	1.0	17.7	1.4	8.60
6	1.2	25.5	1.5	18.80
7	1.9	34.8	1.5	31.70
8	2.2	45.4	1.5	44.70
9	2.3	57.5	1.6	57.70
10	2.25	71.0	1.6	70.60
11	2.2	85.9	1.6	83.80
12	2.1	102.2	1.6	97.90
13	2.0	119.9	1.6	100.00

649
650